Energy Reports 8 (2022) 11429–11439

Contents lists available at ScienceDirect

Energy Reports

journal homepage: www.elsevier.com/locate/egyr

Research paper

A control algorithm to increase the efficient operation of wind energy conversion systems under extreme wind conditions

Nyam Jargalsaikhan [a], Hasan Masrur [a], Atif Iqbal [b,*], Shriram S. Rangarajan [c], Sergelen Byambaa [d], Tomonobu Senjyu [a]

[a] Graduate School of Science and Engineering, University of the Ryukyus, 903-0213, Okinawa, Japan
[b] Department of Electrical Engineering, Qatar University, Qatar
[c] Department of Electrical and Electronics Engineering, SR University, Warangal 506001, India
[d] School of Power Engineering, Mongolian University of Science and Technology, 14191, Ulaanbaatar, Mongolia

ARTICLE INFO

Article history:
Received 12 April 2022
Received in revised form 2 August 2022
Accepted 24 August 2022
Available online 15 September 2022

Keywords:
Wind energy conversion system
PMSG
FCS-MPC
Pitch angle control
Strong wind speed region

ABSTRACT

This paper aims to increase the power production of gearless permanent magnet synchronous generator (PMSG) based wind energy conversion systems (WECS) in strong (greater than 25 m/s) wind speed regions. In general, most wind turbines cut off when wind speed is over the cut-out rate; as a result, the power generation of the wind farm decreases. This study introduces the look-up table pitch angle and rotational speed control to generate extra power in a strong wind region. Consequently, WECS can produce electric power at a reduced level until the wind speed reaches 35 m/s and the possibility of shutting down the wind turbines decreases. The proposed algorithm decreases the mechanical stress of wind turbine by decelerating rotational speed rather than turbine torque in strong wind regions. Furthermore, the model predictive control (MPC) is proposed to replace the PI controller in the inner current loop of the rotor speed control loop, thereby improving the performance of the stator current track. The proposed control method is validated in Matlab/SimPowerSystem software. The simulation result confirms that the proposed control method reduces the possibility of shutdown and guarantees temporally power production in strong wind conditions.

1. Introduction

Over the last two decades, global wind energy capacity has proliferated and become the fastest developing renewable energy technology (Alizadeh and Yazdani, 2013). The early technology used in wind turbines was based on squirrel-cage induction generators (SCIGs) directly connected to the grid. Recently, the technology has developed toward variable speed. The controllability of the wind turbines becomes more and more important as the power level of the turbines increases (Ghedamsi and Aouzellag, 2010). Basically, two types of wind turbines are used in the wind energy conversion system (WECS), such as variable-speed (VS) and fixed-speed (FS) wind turbines (WT) (Abo-Khalil et al., 2020). The VSWTs have many benefits, such as maximum power point tracking (MPPT), better performance, and power output. Now, the PMSG based WECS has several advantages, including 100% variable speed operation, independent active power and reactive power control and excellent smooth grid connection (Yaramasu et al., 2017). The basic diagram of the PMSG based WECS is illustrated in Fig. 1. The machine-side converter (MSC) regulates the rotational speed, active power as well as electromagnetic torque of the generator. The grid-side converter (GSC) is responsible for delivering active and reactive power to the grid, and it also maintaines the voltage stability at the DC-link.

Studies of wind turbine collapse in Chou and Tu (2011), Chou et al. (2019) confirm that strong wind is one primary reason that wind turbines fall down. However, protection mechanisms are expected to protect wind turbines in windstorm conditions to decrease damage. Strong winds can affect the power generation on the wind turbine (Chou et al., 2013). Typhoons and tornadoes cause wind farm supply to fail. If these farms do not have backup power, the protection mechanism (pitch and yaw control system) may fail, and the related system may not communicate with the wind turbine monitoring center. Therefore, wind farm operation and wind turbine status cannot be collected, causing wind turbines under high risk situation. The operation of wind turbines at such high wind speeds is essential. Otherwise, such high wind speeds are uncommon, so designing wind turbines to withstand such high loads is unnecessary (Lumbreras et al., 2014). However, the IEC-61400 standard specifies that the large wind turbines must withstand wind speeds of at least 70 m/s.

On the other hand, repeated cut in and cutouts can reduce the reliability, safety and power generation of wind turbines,

* Corresponding author.
E-mail address: atif.iqbal@qu.edu.qa (A. Iqbal).

https://doi.org/10.1016/j.egyr.2022.08.243

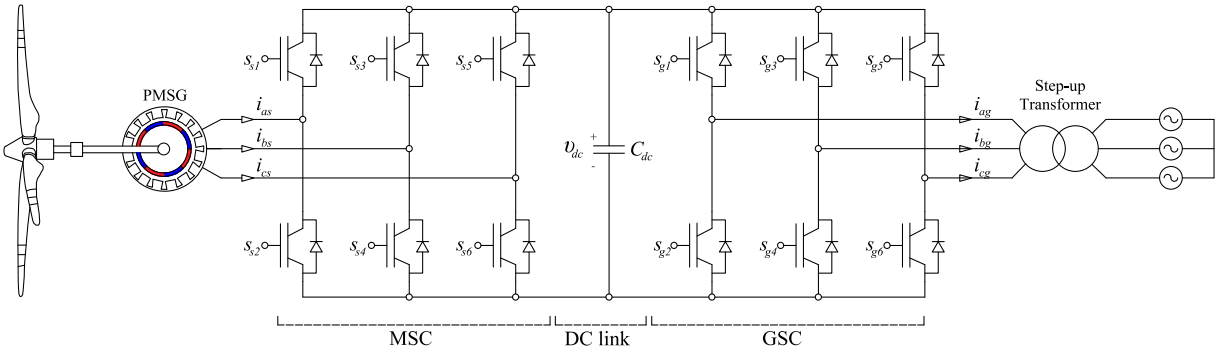

Fig. 1. Basic block diagram of the PMSG based WECS.

especially in strong winds. In Su et al. (2017), the wind turbine control algorithm that prevents repeated cutouts in catastrophic wind conditions is introduced and suggested that number of cutout should be minimized as much as possible. In the standard method, the control purpose of variable speed wind turbine in low wind speeds is to increase energy production. This is generally attained by pitching the blades at the optimal angle and regulating the rotational speed with the electromagnetic torque of the generator. Moreover, it is required to restrict the output power and rotating speed to its rated value or within an acceptable range during high winds. This is typically done by using the generator torque to remain constant while rotational speed is regulated by controlling the pitch angle of the blades (Rezaeiha et al., 2017).

At certain wind speeds, loads on the wind turbine are exceedingly increased, whereby the cost of material necessary to tolerate such loads would be more than the earnings from power production in strong wind conditions. For that reason, it is common in practice to shut down and brake the wind turbine if such a strong wind speed occurs (Wang et al., 2014). This process can lead to the sudden shutdown of an entire wind farm, leading to the oscillation of power grid. Therefore, to increase power generation and guarantee the regular operation of WECS, an efficient control method has been developed in this study. A typical power curve is defined by three wind speed regions: cut-in, rated, and cut-out wind speed, as described in Fig. 2. The cut-in wind speed is the wind speed at which the turbine begins to operate and produce active power (Lydia et al., 2013). The blade should be able to capture enough power to offset the turbine power losses. The rated wind speed is the speed at which the system produces rated power, which is also the rated output power of the generator. The cut-out wind speed is the maximum wind speed at which the turbine can operate before it is shut off (Ali et al., 2019). The turbine is stopped when wind speed passes its cut-out value, preventing damage from excessive wind. However, the sudden shutoff of wind turbines causes instability of the power grid, which needs to be avoided.

In the literature, several studies on the operation of WT in strong wind regions have been reported (Feng and Sheng, 2014; Markou and Larsen, 2009). In Feng and Sheng (2014), the control algorithm for a 2MW wind turbine in the wind speed up to 40 m/s is proposed. The reference power, rotational speed and pitch angle are redesigned to control the wind turbine in high wind conditions. To mitigate the fatigue load on the blade, pitch angle control is proposed for variable speed pitch regulated wind turbines. In Markou and Larsen (2009), the storm control strategy is introduced to generate electric power for a pitch regulated variable speed 2MW turbine in storm conditions in which wind speeds reach 50 m/s. The power-speed regulation and load reduction damper controller for fore-aft and side-to-side tower loads are proposed. Fundamentally, only pitch control is proposed in combination with constant generator torque in over-rated wind speed and variable speed operation in under-rated wind speed in combination with constant speed just below the rated power. The wind turbine runs at a pitch angle of up to 60–70 degrees, which means the pitch angle is noticeably higher, at 50 m/s, to decrease the aerodynamic force.

In article (Jelavić et al., 2013), a control method that allows operating wind turbines in extreme wind speed conditions has been studied. During the wind turbine's operation in high wind speeds, active power and rotational speed reference values are predicted online; therefore, this control method manages the maximum load and mitigates stress on the wind turbine and pitch actuator. Furthermore, in high wind speed regions, only pitch angle control is activated to limit the aerodynamic power and rotating speed of the wind turbine. However, it may increase the mechanical load on the wind turbine blade. All the articles that were mentioned above applied only pitch angle control in the high wind speed region, and mostly PI controllers are used to control wind generators and wind blades. The different types of advanced control systems of WECS in high wind speed region is reported in Colombo et al. (2020), Jiao et al. (2021), Civelek (2020). In article (Colombo et al., 2020), robust sliding mode control (SMC) is proposed to regulate rotational speed under WT model uncertainty. In the (Dahbi et al., 2018), intelligent neural network controller is used to control wind turbine generators, whereas (Viveiros et al., 2015) employs two different advanced control systems such as the fuzzy proportional–integral (Fuzzy PI) and the MPC system for load reduction. Full state feedback control system is proposed in Njiri et al. (2019) to mitigate fatigue load and to extend the lifetime of wind turbine.

In recent years, several different types of model predictive control (MPC) have been applied to address wind turbine control issues (Lio et al., 2014). Due to its fast-transient response, easy implementation, and ability to handle multiple control objectives and constraints, the MPC has been employed in a wide range of power electronic applications (Milev et al., 2020b). Compared to linear control, MPC removes the necessity for a linear PI regulator and modulation stage, and it offers a conceptually different approach for controlling power converters. Therefore, in this study, the MPC is applied to the wind generator current control loop. The control performance obtained by the MPC is significantly determined by the discrete-time (DT) system model, which requires an accurate mathematical model of the wind turbine, generator and power converter. Various studies are found in the literature to obtain a mathematical model of WECS for implementing an MPC strategy (Yaramasu, 2014; Klauco, 2012; Gosk, 2011; Yaramasu and Wu, 2016). It is believed that these research studies provide a more detailed presentation of the accurate model of wind turbine.

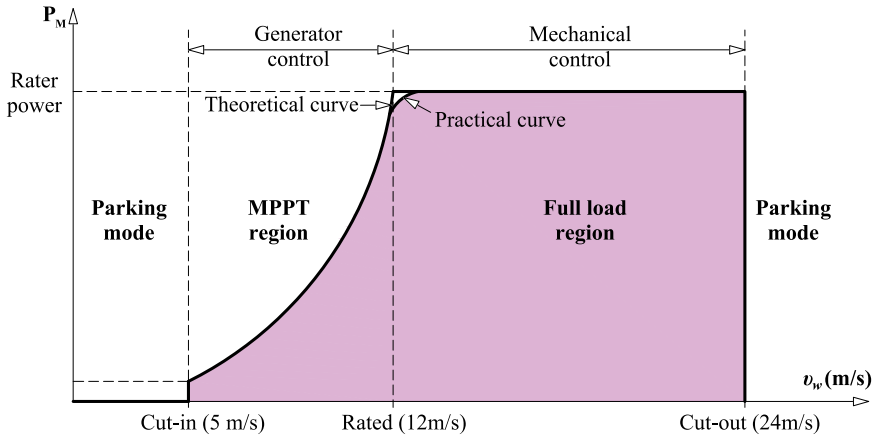

Fig. 2. Conventional output power curve of wind turbine.

Considering the demerit of halting wind turbines in strong wind conditions, this paper introduces the efficient control of the PMSG based WECS in above the cut-out wind speed.

To generate extra power from WT in the strong wind region, a new operating region, referred to as operating region 4, is developed in which the rotational speed and output power are reduced as wind speed increases. The novelty of this study is that the proposed control method decelerates the rotational speed to reduce mechanical load on wind turbine, not only by aerodynamic control in operating regions 3 and 4. The power control block is introduced in the rotational speed control loop and the look-up table based pitch angle control is also introduced to replace the conventional PI-based pitch system in the pitch angle control loop to extend the operation of the WT. With the proposed control algorithm, the power generation of WT is extended from 25 m/s to 35 m/s of wind speeds. In addition, to improve the performance of the current control of PMSG, the MPC control is also proposed for the generator's current control loop. The performance of the proposed method is verified through the simulation results in Matlab using 2MW gearless PMSG WT. The simulation results clarify that a WECS with a proposed control system increases the power generation and maintains the centrifugal load on the wind turbine and pitch actuator in strong wind regions.

The main contributions of this research are outlined as follows: (1) A control algorithm for the operation of wind turbines in strong wind conditions has been developed. A new operating region (Region 4) is proposed to extend the operation of wind turbine in strong wind region. (2) The look-up table based pitch system is developed. The research paper is organized as follows: Section 2 introduces the problem formulation of wind turbine control. Section 3 develops the mathematical model of WECS and WT for MPC implementation. Section 4 presents the configuration of the proposed control scheme in detail. The conventional and proposed pitch angle systems are shown in Section 5. Section 6 illustrates wind turbine control in strong wind region. Section 7 illustrates the simulation result of the proposed control and the conventional method. Eventually, the conclusion of the research is illustrated in Section 8.

2. Problem formulation and control objective

In this study, three operating regions are presented: Partial load, full load and strong wind conditions as illustrated in Fig. 7. The control objectives within these three operation regions are described as follows:

1. Partial load region (Region 2): The control goal is to optimize output power of wind turbine.
2. Full load region (Region 3): the control goal is to regulate the output power at the rated value by pitch angle control and rotating speed control. In addition, the rotating speed of the generator is adjusted in Region 3, not remaining at the rated value.
3. Strong wind region (Region 4): Instead of shutting wind turbines down, the control goal is to regulate output power and rotating speed at a reduced level until 35 m/s wind speed.

3. Mathematic model of wind energy conversion system

3.1. Wind turbine model

The aerodynamic power which is captured by the turbine blades can be calculated (Merabet et al., 2012) by:

$$P_m = 0.5\rho A v^3 C_p(\lambda, \beta) \tag{1}$$

where: $C_p(\lambda, \beta)$ is the power coefficient of the wind turbine and the theoretical maximum value is 0.59 according to Betz limit, ρ is air density, $A = \pi R^2$ is sweep area of blade surface, R is a blade radius, v is wind speed.

The wind turbine's mechanical torque and tip speed ratio (TSR) are given by:

$$T_m = \frac{1}{2} C_p(\lambda, \beta)\rho\pi R^3 \frac{v^2}{\lambda} \tag{2}$$

$$\lambda = \frac{\omega_m R}{\upsilon_w} \tag{3}$$

The wind turbine power coefficient C_p is obtained as follows (Yin et al., 2007):

$$C_p = 0.22\left(\frac{116}{\lambda_i} - 0.4\beta - 5\right)\exp^{\frac{-12.5}{\lambda_i}} \tag{4}$$

$$\lambda_i = \frac{1}{\frac{1}{\lambda + 0.8\beta} - \frac{0.035}{\beta^3 + 1}} \tag{5}$$

3.2. PMSG model

The dynamic model of a PMSG is obtained fully in a synchronous *dq* rotating frame, representing that no AC states are involved in the model. These reference frames are usually used in the FOC and VOC for controlling the MSC and GSC, respectively, in the WECS application.

The dynamic models of stator voltage is expressed in *dq* frame, which rotates synchronously with magnetic flux as follows (Pillay and Krishnan, 1989):

$$\begin{bmatrix} \upsilon_{sd} \\ \upsilon_{sq} \end{bmatrix} = \begin{bmatrix} R_s & 0 \\ 0 & R_s \end{bmatrix} \begin{bmatrix} i_{sd} \\ i_{sq} \end{bmatrix} + \frac{d}{dt} \begin{bmatrix} \phi_{sd} \\ \phi_{sq} \end{bmatrix} + \begin{bmatrix} 0 & -\omega_r \\ \omega_r & 0 \end{bmatrix} \begin{bmatrix} \phi_{sd} \\ \phi_{sq} \end{bmatrix} \tag{6}$$

where: and i_{sq} are the generator currents in dq reference frame, ϕ_{sd} and ϕ_{sq} are the generator flux linkages in dq reference frame, ω_r is the electrical rotational speed, R_s is the generator winding resistance. The stator flux linkages (Qin et al., 2021) are expressed in dq frame as:

$$\begin{bmatrix} \phi_{sd} \\ \phi_{sq} \end{bmatrix} = \begin{bmatrix} L_{sd} & 0 \\ 0 & L_{sq} \end{bmatrix} \begin{bmatrix} i_{sd} \\ i_{sq} \end{bmatrix} + \begin{bmatrix} \phi_r \\ 0 \end{bmatrix} \tag{7}$$

where: L_{sd} and L_{sq} are the flux linkages in *dq* reference frame, ϕ_r is the rotor flux linkage.

The continuous time (CT) stator current dynamics of PMSG in *dq* reference frame is presented as (Springob and Holtz, 1998):

$$\frac{d}{dt} \begin{bmatrix} i_{sd}(t) \\ i_{sq}(t) \end{bmatrix} = A(t) \begin{bmatrix} i_{sd}(t) \\ i_{sq}(t) \end{bmatrix} + B \begin{bmatrix} \upsilon_{sd}(t) \\ \upsilon_{sq}(t) \end{bmatrix} + W(t) \tag{8}$$

CT matrices are illustrated in terms of rotor electrical speed and parameters of SPMSG (Yaramasu, 2014) as:

$$A(t) = \begin{bmatrix} -\frac{R_s}{L_{sd}} & \omega_r(t) L_{sq} \\ -\frac{\omega_r(t) L_{sd}}{L_{sq}} & -\frac{R_s}{L_{sq}} \end{bmatrix}, B = \begin{bmatrix} \frac{1}{L_{sd}} & 0 \\ 0 & \frac{1}{L_{sq}} \end{bmatrix},$$
$$W(t) = \begin{bmatrix} 0 \\ -\frac{\omega_r(t)\phi_r}{L_{sq}} \end{bmatrix} \tag{9}$$

The active and reactive power which are defined in terms of the *dq*-axis voltages and currents are expressed as:

$$\begin{aligned} P_s &= 1.5(\upsilon_{sd} i_{sd} + \upsilon_{sq} i_{sq}) \\ Q_s &= 1.5(\upsilon_{sq} i_{sd} - \upsilon_{sd} i_{sq}) \end{aligned} \tag{10}$$

The electromagnetic torque is calculated as follows (Morinaga et al., 2013):

$$T_e = 1.5p \left[K_r i_{sq} + (L_{sd} - L_{sq}) i_{sd} i_{sq} \right] \tag{11}$$

where: K_r is rotor flux, L_{sd} and L_{sq} are the dq-axis inductances.

The motion equation of wind generator is defined as follows (BinWu Y. Lang et al., 2011):

$$J \frac{d\omega_e}{dt} = T_m - T_e \tag{12}$$

where: J is the equivalent of inertia of wind turbine and generator.

3.3. Discrete time model of PMSG

Using the forward Euler discretization method, the discrete time (DT) model equivalent to the CT model is obtained. To approximate derivatives, the present sampling instant (k) and future sampling instant (k+1) should be measured and calculated. The approximation of derivatives by the forward finite difference approach is given by the following (Wang et al., 2017) equation:

$$\left\{ \frac{dx(t)}{dt} \right\}_{t=kT_s} \approx \frac{x(kT_s + T_s) - x(kT_s)}{T_s} \tag{13}$$

which is simplified as

$$x(k+1) \approx x(k) + T_s \left(\frac{dx(t)}{dt} \right)_{t=kT_s} \tag{14}$$

The DT dq-axis current dynamics of SPMSG is defined as follows (Milev et al., 2020a):

$$\begin{bmatrix} i^p_{sd}(k+1) \\ i^p_{sq}(k+1) \end{bmatrix} = \Phi(k) \begin{bmatrix} i_{sd}(k) \\ i_{sq}(k) \end{bmatrix} + \Gamma_b \begin{bmatrix} \upsilon^p_{sd}(k) \\ \upsilon^p_{sq}(k) \end{bmatrix} + \Gamma_w(k) \tag{15}$$

where: $\upsilon^p_{sd}(k)$ and $\upsilon^p_{sq}(k)$ are the dq-axis predicted voltages. $\Phi(k)$, Γ_b, $\Gamma_w(k)$ are the DT matrices (Dahbi et al., 2018), determined as follows:

$$\Phi(k) = \begin{bmatrix} 1 - \frac{R_s T_s}{L_{sd}} & \frac{\omega_r(t) L_{sq} T_s}{L_{sd}} \\ -\frac{\omega_r(t) L_{sd} T_s}{L_{sq}} & 1 - \frac{R_s T_s}{L_{sq}} \end{bmatrix}, \Gamma_b = \begin{bmatrix} \frac{T_s}{L_{sd}} & 0 \\ 0 & \frac{T_s}{L_{sq}} \end{bmatrix},$$
$$\Gamma_w(k) = \begin{bmatrix} 0 \\ -\frac{\omega_r(t) K_r T_s}{L_{sq}} \end{bmatrix} \tag{16}$$

where: T_s is sampling time, K_r is rotor flux linkage. Based on the measurement of dc link voltage and switching signals of MSC which considered as control sets, the prediction of the dq-axis generator voltages ($\upsilon^p_{sd}(k)$ and $\upsilon^p_{sq}(k)$) are defined (Yaramasu and Wu, 2016) as follows:

$$\begin{bmatrix} \upsilon^p_{sd}(k) \\ \upsilon^p_{sq}(k) \end{bmatrix} = \upsilon_{dc}(k) \begin{bmatrix} cos\theta_r(k) & sin\theta_r(k) \\ -sin\theta_r(k) & cos\theta_r(k) \end{bmatrix}$$
$$\frac{2}{3} \begin{bmatrix} 1 & -\frac{1}{2} & -\frac{1}{2} \\ 0 & \frac{\sqrt{3}}{2} & -\frac{\sqrt{3}}{2} \end{bmatrix} \begin{bmatrix} s^p_a(k) \\ s^p_b(k) \\ s^p_c(k) \end{bmatrix} \tag{17}$$

where: $s^p_a(k)$, $s^p_b(k)$ and $s^p_c(k)$ are the switching signals of the three phase rectifier for MSC, $\theta_r(k)$ is the rotor position angle.

The purpose of the cost function minimization is to evaluate the minimum error between the predicted and reference value of a control variable with respect to each switching state. Eventually, the cost function is designed to satisfy the control objective and is defined as follows:

$$g_r(k) = \begin{bmatrix} \lambda_{id} \left[i^*_{sd}(k+1) - i^p_{sd}(k+1) \right]^2 + \\ + \lambda_{iq} \left[i^*_{sq}(k+1) - i^p_{sq}(k+1) \right]^2 \end{bmatrix} + f_{limit(i_s)} \tag{18}$$

where: $i^*_{sd}(k+1)$ and $i^*_{sq}(k+1)$ are the extrapolated reference current at (k+1) sampling instant, λ_{id} and λ_{iq} are the weighting factor for dq-axis stator current.

The constraint related terms of the cost function is given as:

$$f_{limit}(i_s) = \begin{cases} \infty & \text{if} \sqrt{i^2_{sd}(k) + i^2_{sq}} > i_{max} \\ 0 & \text{if} \sqrt{i^2_{sd}(k) + i^2_{sq}} < i_{max} \end{cases} \tag{19}$$

If the magnitude of stator current is smaller than the maximum current, $f_{limit}(i_s)$ will be zero. Otherwise, it will be infinity.

4. Control scheme configuration of MSC

The overall control scheme of the WTG is illustrated in Fig. 10 in detail. In this paper, PMSG based WT, in which a three-phase stator is connected to grid by a three-phase power converter, is investigated. ω_m and i_{sabc} are directly measured by the generator for regulation of rotational speed and output power. The i_{sabc} are

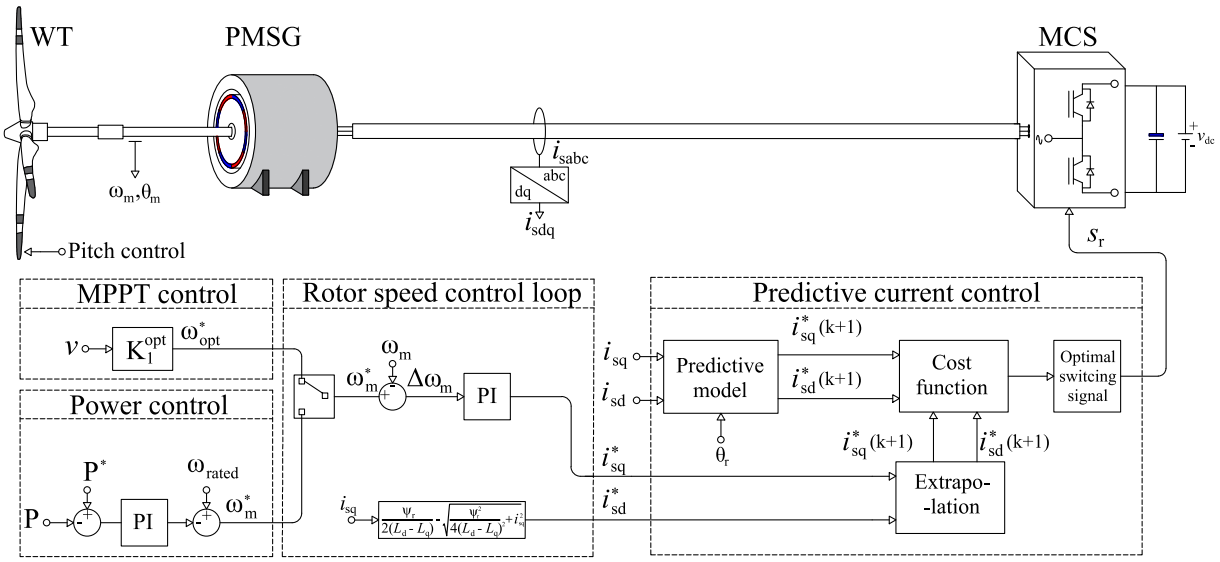

Fig. 3. Configuration of proposed control for MSC of PMSG based WECS.

transformed into the *dq* reference frame through *abc/dq* transformation block. The purpose of GSC is to regulate the DC link voltage at the reference value, and the DC link voltage will be constant during the operation; therefore, GSC is presented as a DC voltage source in this scheme.

In operating region 2, the reference value of rotor speed is calculated by the MPPT control block and rotor speed is regulated at the optimal value (ω^*_{opt}) to generate maximum power from the WTG. The ω^*_{opt} is obtained by optimal tip speed ratio based on the measurement of wind speed ((v) as follows:

$$\omega^*_{opt} = \lambda_{opt} v \tag{20}$$

When WT enters to operating region 3, reference value of rotational speed is calculated by the power control block which reduces the rotational speed to regulated output power. The measured power (P) is subtracted from its reference value (P*) and the error is sent to the PI regulator. The output of this PI controller is then subtracted from rated rotational. As a result of this, the reference rotational speed (ω^*_m) is calculated in operating regions 3 and 4. In the rotational speed control loop, the measured rotational speed is compared to its reference value and error is sent to the PI controller that generator *q*-axis stator current (i^*_{sq}). This controller provides the desired *q*-axis current to manipulate the generator torque, which results in adjusting the rotational speed of the generator at its reference value. The reference power P* is set to its rated value (2WM) in region 3 (see Fig. 3). The reference output power is reduced as a preset power curve in region 4 as shown in Fig. 7.

The DC link voltage v_{dc}, generator three-phase stator current i_{sabc}, mechanical rotational speed, and rotor position angle θ_m are measured to design the MPC controller in current control loop. Based on the measured variables and wind generator parameters, the predictive control block computes the prediction of *dq*-axis current at (k+1) sampling instant. Also, the reference current in the present sample (k) is transformed to (k+1) sampling instant by the extrapolation block. After that, the cost function block evaluates the optimal switching signal that minimizes the error between predicted and extrapolated currents. Then the optimal switching signal is sent to power converter.

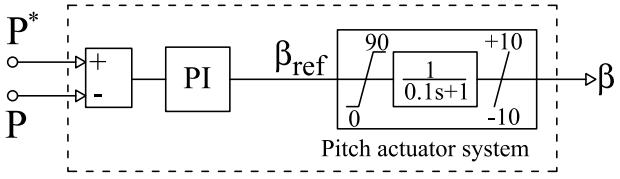

Fig. 4. The standard pitch angle control scheme.

5. Pitch angle control system

5.1. Conventional PI based pitch angle control system

This section introduces two different pitch angle control strategies. Most wind turbines pitch the blades to restrict output power while the rotational speed of turbine remains constant in high wind speed regions. Fig. 4 illustrates the conventional pitch angle scheme.

The conventional control system determines the pitch angle reference using PI controller, which is the error between reference power (P*) and measured power (P*) and this error is sent to the pitch actuator. The pitch actuator is regarded as a hydraulic servo system. Due to the physical restriction of the servo system as well as wind blades, pitch regulation rates are restricted under value of $\pm 10^0$/s. In order to operate wind turbines in strong wind regions, new pitch angle control system will be needed. Therefore, the following subsection will discuss the proposed pitch control system that permits the WT to operate in strong wind regions.

5.2. Look-up table based pitch angle control system

The proposed pitch scheme is depicted in Fig. 5, and Fig. 6 shows the preset pitch angle reference value in operating region 3 and 4.

When a wind turbine moves to the operating region 3 from 2, the pitch angle is determined by the look-up table. This gives fast regulation of pitch angle compared to conventional pitch systems. The pitch value is correlated with wind speed and is designed to decelerate rotational speed instead of keeping it constant at the rated speed. When WTG enters operating region 4 (wind speed is greater than 25 m/s), the rotational speed is already

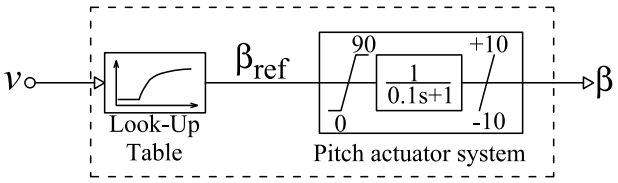

Fig. 5. The proposed pitch angle control.

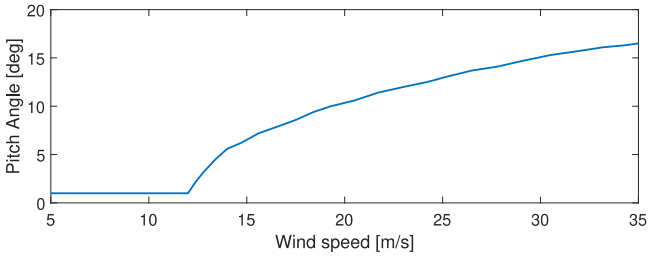

Fig. 6. The preset pitch angle curve with wind speed.

Table 1
Reference output power calculation in all operating regions.

Reference output power	Operating regions
P_s	→ Region 1
$0 < P_s < P_{rated}$	→ Region 2
$P_s = P_{rated}$	→ Region 3
$P_s = \frac{P_{rated}}{1+\exp(-(27.0291-0.8994v))}$	→ Region 4

Table 2
Simulation parameters.

Parameter of wind turbine	
Blade radius R	39 m
Rated wind speed υ_{rated}	12 m/s
Air density ρ	1.205 m/kg^3
Optimal tip speed ratio λ_{opt}	7.461
Parameter of wind generator	
Rated output power P_{rated}	2 MW
Stator resistance R_s	0.005 mohm
dq-axis inductances, $L_{sd} = L_{sq}$	5.5 mH
Pole pairs p	11
Rotor flux ϕ_r	136.25 V s/rad
Equivalent inertia J	10000 kgm^2
Sample time T_s	25 μs

reached at a reduced level. In addition, the reduction of rotational speed requires a small pitch angle, which maintains the balance of stresses due to centrifugal force.

6. The control and operation of WTG in strong wind region

Fig. 7 illustrates the power curve with the new operating region. The proposed power curve provides the same output power as a typical wind turbine in operating regions 1, 2 and 3. Unlike conventional control methods, WTG with the proposed power curve continues power generation at a reduced level in region 4. According to the study of power extension, the extension of the power curve above the cut-out wind speed should be gradually reduced until a new cut-out wind speed is reached. Therefore, the output power in operating region 4 is regulated and designed at a reduced level so that stress does not exceed the maximum value.

The major stresses on the turbine are aerodynamic loads on the blade and centrifugal force. Specifically, the centrifugal force is defined as the product of the square of the rotational speed and the wind velocity, which always acts radial outward, consequently raising load demands at higher tip speeds. For this reason, the proposed method decelerates the rotational speed instead of the mechanical torque during region 4. As a result, the acceptable conditions for generating power can provisionally reach the wind speed of 25 m/s to 35 m/s. In other words, the power production is maintained until the average wind speed over 10 min exceeds 30 m/s or the average wind velocity over 3 s exceeds 35 m/s, which helps to extend the power production of WTG. In addition, the pitch actuator activity is reduced due to the reduction of rotational speed. This causes a provisionally reduced stress on the pitch actuator. The reference output power calculation in all operating regions is given in Table 1:

As illustrated in Table 1, the output power of wind turbines in operating region 4 is calculated by the logistic equation. The reduction of output power needs to be smooth to avoid sudden increases in generator torque; thus, the generator will be under severe thermal stress. Fig. 8 shows the rotating speed of a wind turbine with wind speed. The black line depicts the rotating speed curve using the traditional method, while the blue line depicts the rotating speed curve using the proposed control method. It demonstrates that when the generator enters operating regions 3 and 4, the rotating speed slows, ensuring safe operation in high wind conditions. The proposed control system drives to stop the wind turbine more easily due to the reduction of rotational speed.

7. Simulation result and discussion

In this paper, the non-salient pole PMSG is considered. A hydraulic servo system is used as the pitch angle electric drive. This drive system has a 0.1 s time delay, and the operating speed is $\pm 10^0$/s. Table 2 illustrates the parameters of the wind turbine generator. Fig. 9 illustrates the wind speed profile to confirm the performance of the proposed control system in the strong wind region. At 31 s in the linear wind speed profile, wind speed reaches its cut-out value for wind turbine as shown in Fig. 9a. The wind turbine with a conventional control method shuts down at that moment. On the other hand, the wind turbine with the proposed control method will avoid cutting off and continue generating power.

Operation of wind turbine in linear wind condition

Figs. 10 and 11 show the simulation results of PMSG based WT operation using conventional and proposed control methods at linear wind speed, respectively. These results differentiate the advantages and disadvantages of the conventional and proposed control methods.

Fig. 10a presents the generator's output power using the conventional control method in all operating regions. In region 2, between 0–11 s, the MPPT control is activated to generate maximum power from wind turbines. The features of this region from the control point of view are that the pitch angle will be constant (2^0) during this operating region (Fig. 10d), and electromagnetic torque is regulated to control the rotor speed at its optimal value (Fig. 10b). When wind speed exceeds the rated wind speed at 11 s, the wind turbine enters operating region 3, in which pitch control is activated to limit output power to its rated value (2MW) while electromagnetic torque and rotor speed are set at their rated value (Fig. 10b, e). When wind speed surpasses the cutout value at 30 s, the wind turbine moves into the operating region 4, also known as "Shutdown". The power generation is stopped ($P_s = 0$), rotor speed of the wind turbine is reduced to zero and pitch angle is set to 90^0. Fig. 10f shows the *d*-axis stator of the PMSG, and because of non-salient pole PMSG, which

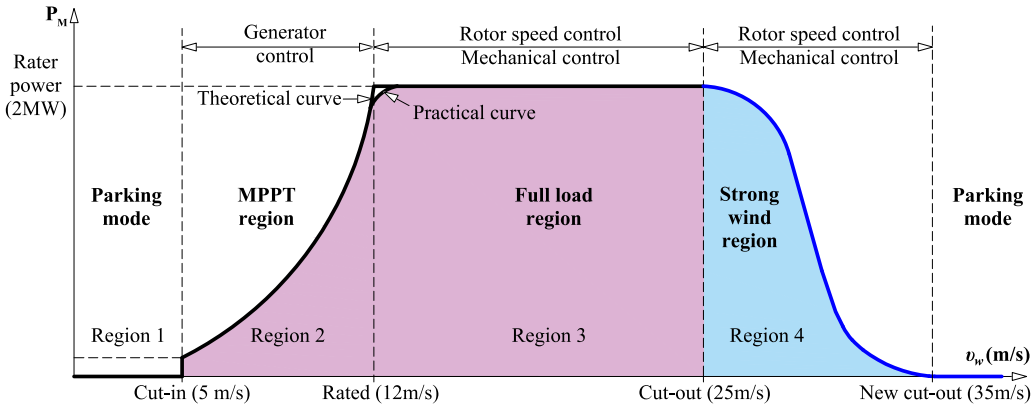

Fig. 7. The proposed output curve of wind turbine.

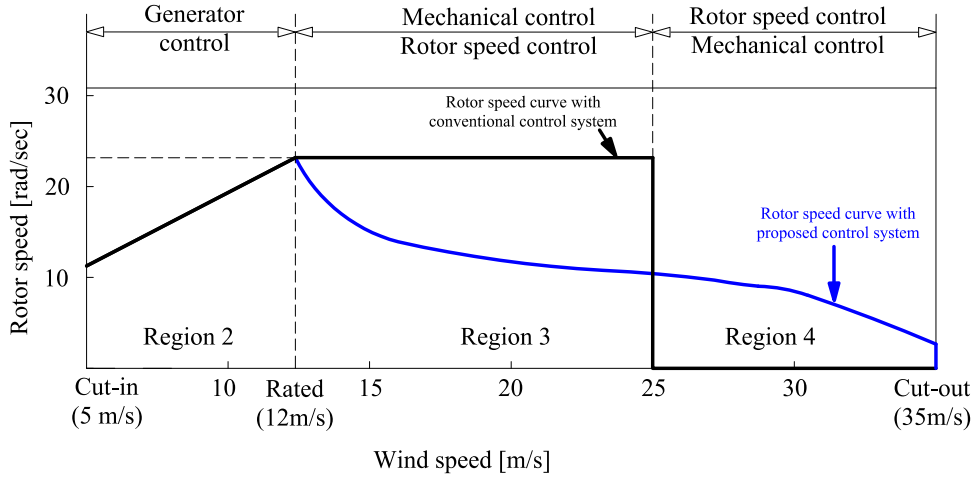

Fig. 8. The rotational speed curve in all operating region.

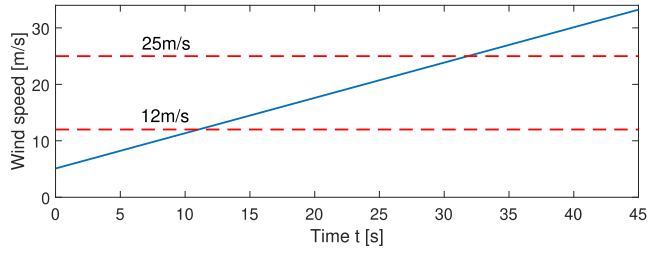

a. Linear wind speed profile

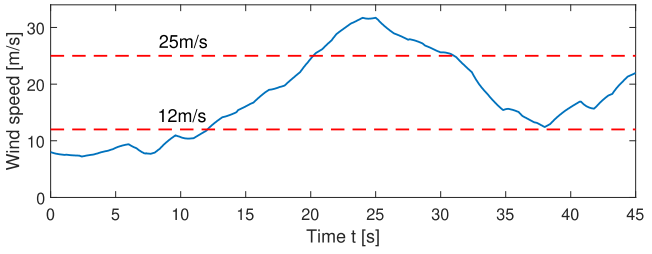

b. Practical wind speed profile

Fig. 9. Wind speed profile which satisfies the all wind speed regions.

$L_{sd} = L_{sq}$ is used in this article, *d*-axis current of the generator needs to be zero to generate maximum torque from the wind generator.

Fig. 10 g illustrates the mechanical torque of wind turbine in all operating regions. In region 2, mechanical torque increases with wind speed, while pitch angle sets its optimal value. When the wind turbine moves to the operating region 3, mechanical torque is limited by the wind turbine blade's position, known as increasing the pitch angle of the blades. In region 4, the mechanical torque of the wind turbine is reduced to zero by the pitching wind turbine blade at 90^0.

Fig. 11 presents the simulation result of a wind turbine using the proposed control method in linear wind speed. The simulation results revealed that the control system guarantees the operation of the wind turbine in region 4.

Fig. 11a illustrates that the wind turbine generates the same output power as the conventional control method in operating regions 2 and 3. When the wind turbine enters operating region 4, the power generation is continued with proposed control rather than the wind turbine being shut down; thus, active power decreases with increasing wind speed and reaches zero at 35 m/s. Fig. 11b depicts the simulation result of the wind turbine's rotating speed. In region 2, rotor speed should be adjusted to the optimal value to generate maximum power at a certain wind speed. The extreme wind conditions cause a potential risk to the wind turbine structure when rotor speed exceeds the rated speed during extreme wind conditions. When wind turbine moves to operating region 3 from 2, power control block takes the control of WT, and the rotational speed is reduced to regulate output power to its reference value in regions 3 and 4. It is considered that rotating speed gradually decreases when wind speed reaches

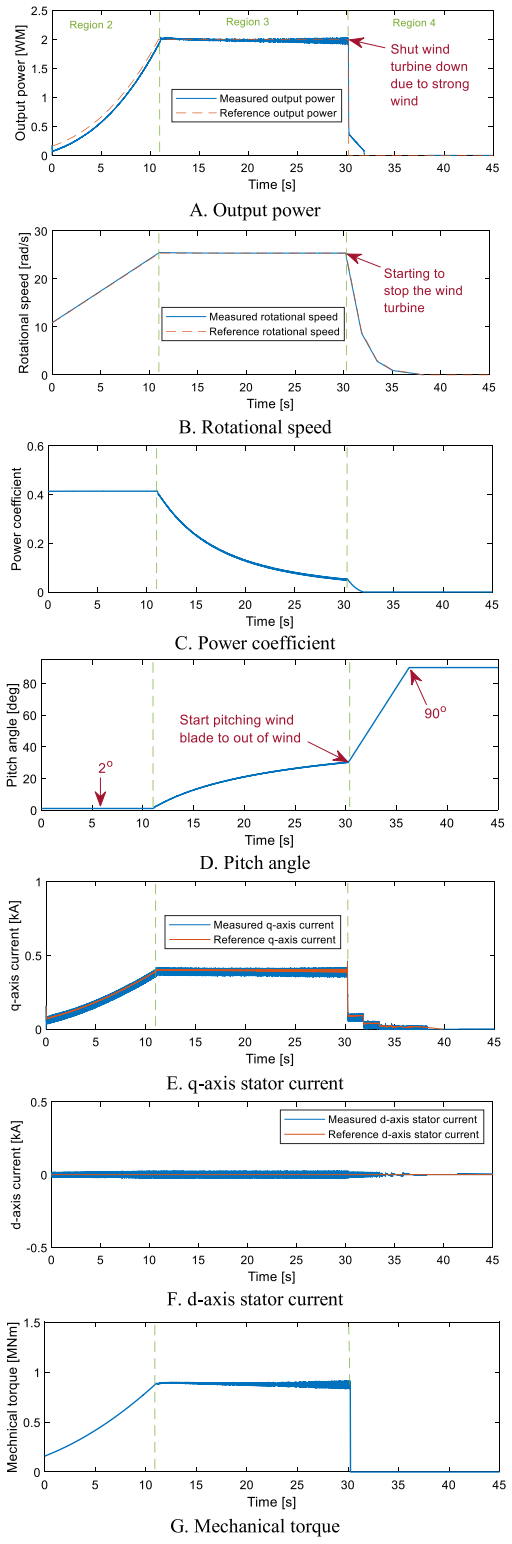

Fig. 10. The simulation result of conventional PI based pitch angle control system in linear wind speed profile.

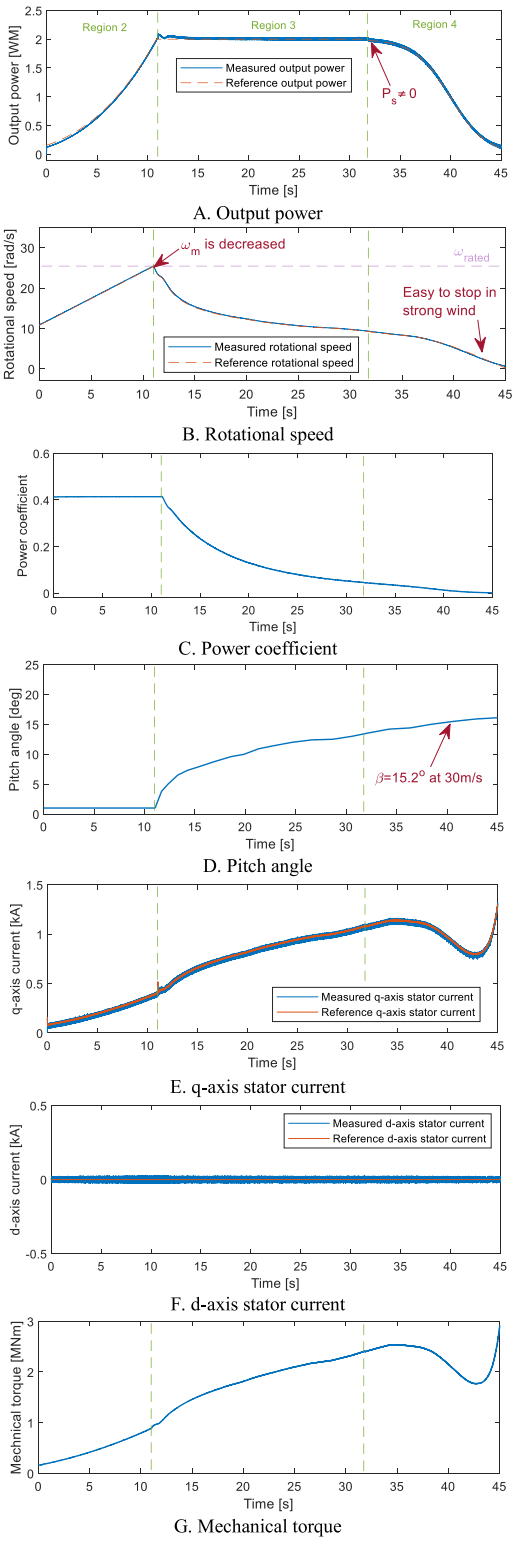

Fig. 11. The simulation result of proposed look-up table based pitch control in linear wind speed profile.

its rated value. The rotational speed reduction lowers the pitch actuator action when the wind turbine operates at a higher wind speed. In addition, the reduction of the rotational speed makes it easier to brake and lock the wind turbine and reduces the centrifugal force on the wind turbine in a strong wind region.

Fig. 11c represents the power coefficient of the wind turbine. The power coefficient should be maximized in region 2 and reduced to limit output power at the optimal value in regions 3 and 4. In the conventional control method, power coefficient regulation is achieved by controlling the pitch angle of the wind

blade, whereas the proposed method controls the power coefficient by regulating both the rotating speed and pitch angle of the wind turbine.

Fig. 11d shows the pitch angle of the wind turbine, and it can be noticed that the wind turbine operates at maximum pitch angles around 15.2^0 at operating regions 3 and 4. It means the proposed control can reduce the activity of the pitch angle. Fig. 11e and 11f illustrate the *dq*-axis stator current. It can be considered that the actual *dq*-axis current follows the reference value with good performance. The electromagnetic torque is controlled to regulate the rotational speed at its optimal value and generate maximum power from the wind generator. According to Eq. (11), the control of electromagnetic torque is achieved by controlling the *q*-axis current. In Fig. 10g, the mechanical torque of the wind turbine is depicted, and it shows that when wind speed passes 25 m/s at 31.5 s, the mechanical torque of the wind turbine is brought down, leading to a reduction of mechanical stress on the wind turbine.

Operation of wind turbine in practical strong wind condition

Fig. 9b shows the wind speed profile. The wind speed exceeds the wind turbine's cut-out value between 20.1 s and 30.1 s. Figs. 12 and 13 illustrate the simulation result of conventional and proposed control method, respectively. The active power of WTG is depicted in Figs. 12a and 13a.

When wind speed passes its maximum value, the wind turbine with the conventional control method shuts down, and output power becomes zero, as shown in Fig. 12a. In Fig. 13a, wind speed is over its rated value in region 3; therefore, pitch angle control and rotational speed control are activated to limit output power to its reference value. The rotor speed is regulated to track output power at its reference value by controlling the electromagnetic torque. It is clear that the output power reference remains constant while the rotor speed of the wind turbine is decelerated to regulate the output power of the wind generator in region 3. The wind speed passes from 25 m/s to 20.1 s; therein, the power generation and rotational speed of the generator decrease, corresponding to the wind speed increases in the proposed control method. Instead of shutting the wind turbine, the proposed control can generate electric power from the wind generator in region 4.

Figs. 12b and 13b depict the simulation results of the wind turbine rotor speed. In region 2, rotor speed should be adjusted to the optimal value to generate maximum power at a certain wind speed. The extreme wind condition causes a potential risk to the wind turbine structure when rotor speed exceeds the rated speed during extreme wind conditions. The rotation speed is reduced to regulate output power to its reference value in regions 3 and 4. It is considered that rotating speed gradually decreases when wind speed reaches its rated value. The turbulent wind condition which causes to overspeed of wind turbine, leads to unnecessary shutdown in strong wind condition. However, in order to evaluate the full effects of turbulent conditions on wind turbine structure and operation, further study will be conducted. Figs. 12c and 13c illustrate the power coefficient of the wind turbine. When the wind turbine operates in region 2, the power coefficient is constant at its maximum value. Then it moves to operate regions 3 and 4, which reduce to limit mechanical power. The pitch angle of the wind turbine is illustrated in Figs. 12d and 13d. The proposed method reduces the pitch angle action in operating regions 3 and 4, whereas the wind turbine with the conventional control method is shut down and the pitch angle is set at 90°. Figs. 12e, 13e, 12f and 13f illustrate the *dq*-axis stator currents, respectively. *d*-axis current is set to 0 during the operation. However, *q*-axis current is controlled to regulate the electromagnetic torque during all operating regions.

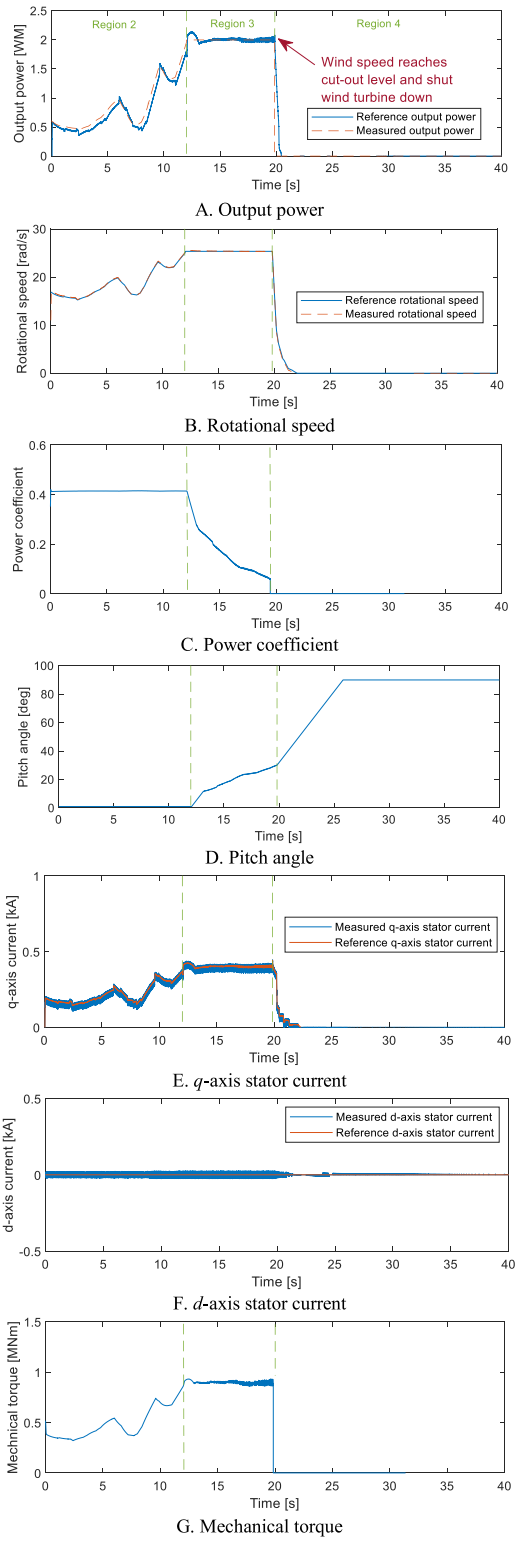

Fig. 12. The simulation result of conventional PI based pitch angle control system in practical wind profile.

8. Conclusion

This paper introduces the control algorithm to increase the power production of PMSG based WECS in strong wind regions. The conventional method is compared with the proposed method

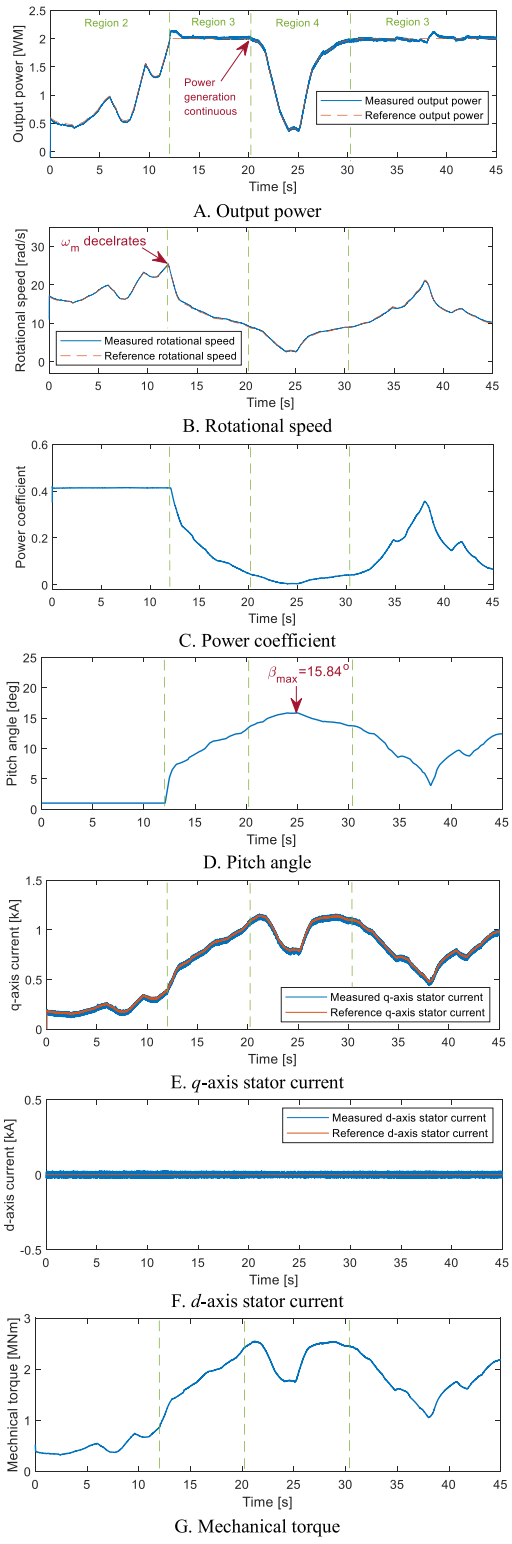

Fig. 13. The simulation result of proposed look-up table based pitch control in practical wind profile.

considering the same operating conditions and system parameters. The rotational speed and look-up table based pitch angle control systems are introduced to adjust the rotational speed and regulate the output power of the generator in regions 3 and 4. From the results, both control systems perform similarly in operating region 2. In operating region 3, the proposed control reduces the rotational speed to regulate output power which causes the rotational speed to decelerate, whereas conventional control maintains the rotational speed at the rated value. Then WT enters operating region 4; the proposed control system reduces the active power and rotational speed with a specific value, whereas conventional control shuts down the wind turbine. The proposed control continues power generation without a sudden shutdown. On the other hand, the conventional control method stops power generation. Plus, under the proposed control, pitch actuator action and high-aggressive aerodynamic behavior of wind turbine can be reduced. The wind turbine with the proposed control is able to generate power at up to 35 m/s, thereby increasing the power production of WT. However, if wind velocity is greater than 35 m/s, wind turbines are shut down and stopped. Also, the tower dynamics, which is one of the major issues in strong wind conditions, is not considered in this research. Therefore, further research will be done regarding the tower dynamics of WT.

CRediT authorship contribution statement

Nyam Jargalsaikhan: Conceptualization, Methodology, Investigation, Software, Validation, Visualization, Writing - original draft, Writing - review & editing. **Hasan Masrur:** Data curation, Investigation, Project administration, Resources, Writing - original draft, Writing - review & editing. **Atif Iqbal:** Supervision, Funding acquisition. **Shriram S. Rangarajan:** Visualization. **Sergelen Byambaa:** Software, Data curation. **Tomonobu Senjyu:** Validation, Supervision.

Declaration of competing interest

The authors declare that they have no known competing financial interests or personal relationships that could have appeared to influence the work reported in this paper.

Data availability

No data was used for the research described in the article.

Acknowledgments

This publication was made possible by Qatar University Collaborative Research grant [QUCG-CENG-21/22-1] from the Qatar University. The statements made herein are solely the responsibility of the authors. The APC for this article is funded by the Qatar National Library, Doha, Qatar.

References

Abo-Khalil, A.G., Eltamaly, A.M., Praveen, R.P., Alghamdi, A.S., Tlili, I., 2020. A sensorless wind speed and rotor position control of pmsg in wind power generation systems. Sustain. 12 (20), 1–19. http://dx.doi.org/10.3390/su12208481.

Ali, M.A.S., Mehmood, K.K., Kim, C.H., 2019. Full operational regimes for SPMSG-based WECS using generation of active current references. Int. J. Electr. Power Energy Syst. 112 (May), 428–441. http://dx.doi.org/10.1016/j.ijepes.2019.05.028.

Alizadeh, O., Yazdani, A., 2013. A strategy for real power control in a direct-drive PMSG-based wind energy conversion system. IEEE Trans. Power Deliv. 28 (3), 1297–1305. http://dx.doi.org/10.1109/TPWRD.2013.2258177.

BinWu Y. Lang, Zargari, N., Kouro, S., 2011. Power Conversion and Control of Wind Energy Systems, first ed. John Wiley & Sons, Inc. Hoboken, New Jersey., p. 481.

Chou, J.S., Chiu, C.K., Huang, I.K., Chi, K.N., 2013. Failure analysis of wind turbine blade under critical wind loads. Eng. Fail. Anal. 27, 99–118. http://dx.doi.org/10.1016/j.engfailanal.2012.08.002.

Chou, J.S., Ou, Y.C., Lin, K.Y., 2019. Collapse mechanism and risk management of wind turbine tower in strong wind. J. Wind Eng. Ind. Aerodyn. 193 (July), 103962. http://dx.doi.org/10.1016/j.jweia.2019.103962.

Chou, J.S., Tu, W.T., 2011. Failure analysis and risk management of a collapsed large wind turbine tower. Eng. Fail. Anal. 18 (1), 295–313. http://dx.doi.org/10.1016/j.engfailanal.2010.09.008.

Civelek, Z., 2020. Optimization of fuzzy logic (takagi–sugeno) blade pitch angle controller in wind turbines by genetic algorithm. Eng. Sci. Technol. Int. J. 23 (1), 1–9. http://dx.doi.org/10.1016/j.jestch.2019.04.010.

Colombo, L., Corradini, M.L., Ippoliti, G., Orlando, G., 2020. Pitch angle control of a wind turbine operating above the rated wind speed: A sliding mode control approach. ISA Trans. 96, 95–102. http://dx.doi.org/10.1016/j.isatra.2019.07.002.

Dahbi, A., Reama, A., Maouedj, R., Berbaoui, B., Adel, M., 2018. Analysis and control of the wind turbine in different operation modes. In: Proceedings of 2018 6th International Renewable and Sustainable Energy Conference, Vol. 85, no. 6. IRSEC 2018, http://dx.doi.org/10.1109/IRSEC.2018.8702977.

Feng, J., Sheng, W.Z., 2014. Operating wind turbines in strong wind conditions by using feedforward-feedback control. J. Phys. Conf. Ser. 555 (1), http://dx.doi.org/10.1088/1742-6596/555/1/012035.

Ghedamsi, K., Aouzellag, D., 2010. Improvement of the performances for wind energy conversions systems. Int. J. Electr. Power Energy Syst. 32 (9), 936–945. http://dx.doi.org/10.1016/j.ijepes.2010.02.012.

Gosk, A., 2011. Model Predictive Control of a Wind Turbine. Technical University of Denmark.

Jelavić, M., Petrović, V., Barišić, M., Ivanović, I., 2013. Wind turbine control beyond the cut-out wind speed. EWEC 2013, pp. 343–349,

Jiao, X., Yang, Q., Xu, B., 2021. Hybrid intelligent feedforward-feedback pitch control for VSWT with predicted wind speed. IEEE Trans. Energy Convers. 36 (4), 2770–2781. http://dx.doi.org/10.1109/TEC.2021.3076839.

Klauco, M., 2012. Model Predictive Control of Wind Turbines. Technical university of Denmark.

Lio, W.H., Rossiter, J.A., Jones, B.L., 2014. A review on applications of model predictive control to wind turbines. In: 2014 UKACC Int. Conf. Control. Control 2014 - Proc., No. July. pp. 673–678. http://dx.doi.org/10.1109/CONTROL.2014.6915220.

Lumbreras, C., Guerrero, J.M., García, P., Briz, F., Díaz, D., 2014. Control of a small wind turbine in the high wind speed region. In: 2014 IEEE Energy Convers. Congr. Expo.. ECCE 2014, pp. 4896–4903. http://dx.doi.org/10.1109/ECCE.2014.6954072.

Lydia, M., Selvakumar, A.I., Kumar, S.S., Kumar, G.E.P., 2013. Advanced algorithms for wind turbine power curve modeling. IEEE Trans. Sustain. Energy 4 (3), 827–835. http://dx.doi.org/10.1109/TSTE.2013.2247641.

Markou, H., Larsen, T.J., 2009. Control strategies for operation of pitch regulated turbines above cut-out wind speeds. Eur. Wind Energy Conf. Exhib. 2009, EWEC 2009 6 (December 2014), 4288–4297.

Merabet, A., Rajasekaran, V., Kerr, J., 2012. Modelling and control of a pitch controlled wind turbine experiment workstation. In: IECON Proc. (Industrial Electron. Conf.), No. 1. pp. 4316–4320. http://dx.doi.org/10.1109/IECON.2012.6389195.

Milev, K., Yaramasu, V., Dekka, A., Kouro, S., 2020a. Modulated predictive current control of PMSG-based wind energy systems. In: 2020 11th Power Electron. Drive Syst. Technol. Conf.. PEDSTC 2020, pp. 1–6. http://dx.doi.org/10.1109/PEDSTC49159.2020.9088365.

Milev, K., Yaramasu, V., Dekka, A., Kouro, S., Dragicevic, T., Rodriguez, J., 2020b. Modulated model predictive torque and power control of gearless PMSG wind turbines. In: 2020 IEEE 11th Int. Symp. Power Electron. Distrib. Gener. Syst.. PEDG 2020, pp. 352–357. http://dx.doi.org/10.1109/PEDG48541.2020.9244307.

Morinaga, S., Izumi, Y., Howlader, A.M., Yona, A., Senjyu, T., Funabashi, T., 2013. Output power control of a PMSG based wind turbine in strong wind conditions. In: IEEE Int. Symp. Ind. Electron., No. 1. http://dx.doi.org/10.1109/ISIE.2013.6563765.

Njiri, J.G., Beganovic, N., Do, M.H., Söffker, D., 2019. Consideration of lifetime and fatigue load in wind turbine control. Renew. Energy 131, 818–828. http://dx.doi.org/10.1016/j.renene.2018.07.109.

Pillay, P., Krishnan, R., 1989. Modeling, simulation, and analysis of permanent-magnet motor drives, Part I: The permanent-magnet synchronous motor drive. IEEE Trans. Ind. Appl. 25 (2), 265–273. http://dx.doi.org/10.1109/28.25541.

Qin, S., Chang, Y., Xie, Z., Li, S., 2021. Improved virtual inertia of PMSG-based wind turbines based on multi-objective model-predictive control. Energies 14 (12), 3612. http://dx.doi.org/10.3390/en14123612.

Rezaeiha, A., Kalkman, I., Blocken, B., 2017. Effect of pitch angle on power performance and aerodynamics of a vertical axis wind turbine. Appl. Energy 197, 132–150. http://dx.doi.org/10.1016/j.apenergy.2017.03.128.

Springob, L., Holtz, J., 1998. High-bandwidth current control for torque-ripple compensation in PM synchronous machines. IEEE Trans. Ind. Electron. 45 (5), 713–721. http://dx.doi.org/10.1109/41.720327.

Su, S., Yin, Z., Yang, H., Hui, X., Alsmadi, Y.M., 2017. Re-cutin control of wind turbines based on a combined dead band of time and wind speed. In 2017 IEEE Industry Applications Society Annual Meeting 1–6. http://dx.doi.org/10.1109/IAS.2017.8101726.

Viveiros, C., Melicio, R., Igreja, J.M., Mendes, V.M.F., 2015. Wind energy conversion system control using distinct controllers for different operating regions. In: 2015 International Conference on Renewable Energy Research and Applications, Vol. 5. ICRERA 2015, pp. 959–964. http://dx.doi.org/10.1109/ICRERA.2015.7418552.

Wang, K., Hansen, M.O.L., Moan, T., 2014. Dynamic analysis of a floating vertical axis wind turbine under emergency shutdown using hydrodynamic brake. Energy Procedia 53 (C), 56–69. http://dx.doi.org/10.1016/j.egypro.2014.07.215.

Wang, F., Mei, X., Tao, P., Kenne, R., Rodriguez, J., 2017. Predictive Field-Oriented Control for Electric Drives, Vol. 3, no. 1. pp. 73–78. http://dx.doi.org/10.23919/CJEE.2017.7961324.

Yaramasu, V.N.R., 2014. Predictive Control of Multilevel Converters for Megawatt Wind Energy Conversion Systems. Ryerson University.

Yaramasu, V., Dekka, A., Durán, M.J., Kouro, S., Wu, B., 2017. PMSG-based wind energy conversion systems: Survey on power converters and controls. IET Electr. Power Appl. 11 (6), 956–968. http://dx.doi.org/10.1049/iet-epa.2016.0799.

Yaramasu, V., Wu, B., 2016. Model predictive control of wind energy conversion systems.

Yin, M., Li, G., Zhou, M., Zhao, C., 2007. Modeling of the wind turbine with a permanent magnet synchronous generator for integration. In: 2007 IEEE Power Eng. Soc. Gen. Meet.. PES, pp. 1–6. http://dx.doi.org/10.1109/PES.2007.385982.